Volume 17
Number 2
Dec 2025

Journal of
The Indonesian Society of Integrated Chemistry
Published by Jambi University, Chemistry Education Study Program

P-ISSN 2085-1715 & E-ISSN 2621-5543

JISIC

# Optimization of Ion-Ligand Stoichiometry in Synthesis of Ionic Imprinted Polymer for Selective Fe(III) Adsorption

**Tazkiya Auliya[1], Maria Monica Sianita Basukiwardojo[2*]**

[1,2] Department of Chemistry, Faculty of Mathematics and Natural Sciences, Universitas Negeri Surabaya, Indonesia

## ABSTRACT

This study investigates the influence of the complex structure formed between the template ion and the ligand on the adsorption efficiency of metal ions by Ionic Imprinted Polymer (IIP). The IIP was synthesized with ion-template/ligand stoichiometric ratios of 1:1, 1:2, 1:3, 1:4, and 1:5 via precipitation polymerization. Materials used in synthesis are $Fe(NO_3)_3$ as the template ion, EDTA as the ligand, MAA as the functional monomer, EGDMA as the cross-linker, and BPO as the initiator. Adsorption experiments confirmed that the IIP prepared with a 1:1 Fe(III)/EDTA ratio exhibited the highest maximum adsorption capacity of 5.18 mg/g, outperforming other stoichiometric compositions. Characterization of the IIP(1:1) using FTIR confirmed the presence of functional groups corresponding to Fe-EDTA interactions in the Non-Imprinted Polymer (NIP), while such interactions were absent in the IIP, indicating successful template removal and the formation of binding cavities suitable for selective metal ion adsorption. EDX analysis also revealed a difference in Fe(III) content, with the NIP at 0.52% and the IIP at 0.36%. Results reveal that the IIP exhibits selective adsorption toward the target ion, indicating its potential for selective metal ion separation and environmental remediation.

Keywords: Adsorption, Complex Ion/Ligand, Fe(III), Ionic Imprinted Polymer

Received: Novemver, 14 2025;
Revised: November, 27 2025;
Accepted: December, 12 2025

* Corresponding author: mariamonica@unesa.ac.id
DOI: https://doi.org/10.22437/10.22437/jisic.v17i2.49889

## INTRODUCTION

Iron is an essential metal required by living organisms for the formation of haemoglobin in the blood. However, excessive intake and long-term accumulation of iron in the body can be harmful and may lead to various diseases (Pramastuti et al., 2024). Iron in aquatic environments generally exists in dissolved forms, namely Fe(II) and Fe(III), which can form colloidal particles and associate with organic or inorganic compounds such as clay particles (Salisna et al., 2021). However, in water, Fe(II) is unstable and tends to precipitate as insoluble Fe(III) hydroxide (Rahman et al., 2024).

Iron in aquatic environments can be removed using several techniques, one of which is adsorption. Adsorption refers to the phenomenon where molecules or particles of

a substance accumulate on the surface of a solid material (known as the adsorbent) as a result of intermolecular attractive forces. In this process, the adsorbent captures the target substance, known as the adsorbate (Kusumaningsih et al., 2022). The adsorption method offers high efficiency across a wide pH range (Raji et al., 2023). Also, adsorption effectively removes metals even at very low concentrations (Macena et al., 2025).

One promising type of adsorbent is the Ion-Imprinted Polymer (IIP). IIPs exhibit high selectivity because they can recognize specific interactions between ions and ligands based on the size and shape of the metal ion (Ishak et al., 2020). The principle of IIP synthesis involves forming a complex between a template ion and a ligand, which is then fixed within a cross-linked polymer matrix, resulting in a Non-Imprinted Polymer (NIP). After removal of the template ion, cavities complementary in shape, size, and functional groups to the template ion are generated within the polymer structure, leading to the formation of IIP (Wirawan et al., 2019). In contrast to NIP, which does not contain recognition cavities, IIP is characterized by the presence of imprinted sites that remain after the template ion has been removed (Cao et al., 2024).

The formation of the complex between the template ion and the ligand is a crucial step in IIP synthesis, as it influences the internal structure of the polymer and its ability to selectively bind metal ions (Iacob et al., 2018). This study aims to investigate how variations in the template ion–ligand ratio affect the adsorption of Fe(III) ions. The analysis enables determination of the metal/ligand complex stoichiometry (1:1; 1:2; 1:3; 1:4; and 1:5) by adjusting the initial molar ratio of metal to ligand in the polymerization mixture. The selective behavior of binding sites in IIPs is strongly affected by their stoichiometric complexity, consequently, this approach is anticipated to improve the overall performance of the synthesized material. Previous studies have reported that an ion template/ligand ratio of 1:2 produced the highest selectivity in Ni(II)/DPC-based IIP systems (Zhou et al., 2017). Similarly, Giove, (2024) found that a 1:2 ratio between Ni(II) and 2,2'-(pyridyl)imidazole yielded the most stable complex. The purpose of comparing different template ion/ligand ratios in this research is to identify the optimal composition for Fe(III) ion adsorption. Ligands in IIPs that do not form complexes with the template ion tend to create non-selective binding sites, similar to those found in NIPs (Fei & Hu, 2022). Accordingly, this research aims to investigate how variations in template ion–ligand composition influence the performance of IIPs, with the objective of developing materials with enhanced ion-separation efficiency.

## RESEARCH METHOD

### Material and Methods

The materials used in this study are $Fe(NO_3)_3$ (Merck), $Na_2EDTA$ (Merck). methacrylic acid (MAA) (Sigma Aldrich), benzoyl peroxide (BPO), ethylene glycol dimethacrylate (Sigma Aldrich)) (Merck), acetonitrile (Merck), ethanol (Merck), distilled water, deionized water, nitrogen gas ($N_2$), nitric acid 65% (Merck), and hydrochloric acid HCl 37% (Merck).

The equipment used in this experiment included a magnetic stirrer, reagent bottles, beaker glass, measuring cylinder, vortex mixer, micropipettes, volumetric flask, thermometer, glass funnel, filter paper, measuring pipette, volumetric pipette, magnetic stirrer, vacuum membrane filtration apparatus, and analytical balance. The metal concentration was analyzed using Atomic Absorption Spectrophotometry (AAS, Shimadzu AA-7000). The characterization of IIP-Fe, NIP-Fe, and blank polymer was performed with

instruments, Fourier Transform Infrared (FTIR, Perkin Elmer Spectrum One) at a wavelength range of 400-4000 $cm^{-1}$, and SEM-EDX (Scanning Electron Microscopy-Energy Dispersive X-ray, ZEISS Evo 10).

**Procedures**

**Synthesis of NIP-Fe(III)**

Non-Imprinted Polymer (NIP) was synthesized using the precipitation polymerization method. The procedure began by mixing $Fe(NO_3)_3$ (0.1 mmol, 0.0404 g) with $Na_2EDTA$ at varying amounts of 0.1 mmol (0.0372 g), 0.2 mmol (0.0744 g), and 0.3 mmol (0.1116 g). To this mixture, 60 mL of a solvent mixture of ethanol and acetonitrile (2:1, v/v) was added, and the solution was stirred on a magnetic stirrer at 600 rpm at room temperature for 30 minutes. Subsequently, BPO (0.2 mmol, 0.0484 g), EGDMA (20 mmol, 3.9644 g), and MAA (0.4 mmol, 340 µL) were added to the mixture and homogenized using a vortex mixer. To eliminate oxygen interference, the solution was purged with nitrogen gas for 5 minutes and covered with aluminum foil. The mixture was magnetically stirred at 800 rpm and 70°C until a paste-like consistency developed. The formed polymer was filtered and washed successively with ethanol and distilled water. The residue was then dried in an oven at 60°C until constant weight, yielding NIP. A blank polymer was synthesized using the same procedure, without the addition of the template ion.

**Determination of Leaching Percentage**

The leaching process involves removing the template ions present in the NIP, resulting in the formation of pores or cavities. The synthesized NIP was leached with 100 mL of 3M $HNO_3$. The residue was separated from the filtrate then washed with distilled water. The obtained residue was then oven-dried at 60°C until constant weight was achieved, yielding the Ion-Imprinted Polymer (IIP). The filtrate from the leaching process and the washing solution were subsequently examined using Atomic Absorption Spectrophotometry (AAS) to quantify the concentrations of dissolved and leached metal ions.

**Determination of Adsorption Capacity**

Adsorption using IIPs with composition ratios of 1:1, 1:2, 1:3, 1:4, and 1:5 was conducted to determine the IIP with the best adsorption performance. Each of the IIP was weighed to 0.05 g and added to 50 mL of Fe(III) standard solution with a concentration of 5 ppm. The adsorption contact time is 2 hours. After stirring, the solutions were filtered, and the metal ion concentrations in the filtrates were analyzed. The Fe(III) standard solution was adjusted to pH 7, corresponding to the optimum pH condition for adsorption. Adsorption capacity was calculated using the following equation:

$$Qe = \frac{(C_i - C_f)V}{m} \quad (2)$$

Qe (mg/g) represents the adsorption capacity, which is calculated based on the initial solute concentration Ci (mg/L), the equilibrium concentration Cf (mg/L), the amount of adsorbent m (g), and the total solution volume V (L).

**Characterization analysis of NIP-Fe(III) and IIP-Fe(III)**

Chemical characterization of NIP and IIP was carried out using FTIR at a wavelength range of 400-4000 $cm^{-1}$ to identify the functional groups. SEM-EDX was used to examine the surface morphology and to determine the elemental composition of the polymer. The blank polymer was also characterized as a reference.

**Fe(III)/Cr(III) Selectivity**

The selectivity determination was carried out using the IIP with the optimal ratio. Approximately 0.05 g of IIP was weighed and added to 50 mL of a 5 ppm Fe(III)/Cr(III) standard solution. The resulting mixture was subjected to magnetic stirring at 800 rpm for 2 hours to achieve adsorption equilibrium. Post-adsorption, the concentrations of Fe(III) and Cr(III) were

quantified. The pH of the standard solution was controlled at nearly 7. Selectivity coefficient, $K_{Cr(III)}^{Fe(III)}$, is calculated according to Eq. (3) (Laatikainen et al., 2015):

$$K_{Cr(III)}^{Fe(III)} = \frac{Qe_{Fe(III)} Qe_{Cr(III)}}{Cf_{Fe}(III) Cf_{Cr(III)}} \quad (3)$$

Qe (mg/g) is defined as the adsorption capacity, and Cf (mg/L) is defined as the final concentration in the solution.

## RESULT AND DISCUSSION

### Leaching Percentage

Metal ions were leached from the polymer's surface and cavities using an $HNO_3$ solution. $HNO_3$ acts not only as a reactive solvent but also as the primary driving force for ion-exchange reactions that facilitate metal leaching through ionic interactions.

As shown in Table 1, the IIP with a 1:1 template-to-ligand ratio exhibited the highest leaching percentage. The elimination of Fe(III) ions in the leaching phase plays a decisive role in shaping both the number and the structural features of the cavities embedded in the polymer matrix. These cavities function as specific recognition sites for the target ion. The results demonstrate that the efficiency of ion removal, as reflected by the leaching percentage, is directly correlated with the degree of cavity formation and, consequently, with the selectivity performance of the IIP.

**Table 1.** Leaching percentage of NIP

| Value | % Leaching |
|---|---|
| NIP(1:1) | 97.43 |
| NIP(1:2) | 94.67 |
| NIP(1:3) | 88.99 |
| NIP(1:4) | 85.18 |
| NIP(1:5) | 75.28 |

### Adsorption Capacity

This study identified a strong correlation between ligand amount and polymer adsorption efficiency. As summarized in Table 2, an elevated ligand concentration was associated with decreased adsorption capacity.

**Table 2.** The adsorption capacity of IIP

| Materials | C*i* (mg/L) | C*f* (mg/L) | Adsorption Capacity (mg/g) |
|---|---|---|---|
| IIP(1:1) | 6.176 | 0.986 | 5.17 |
| IIP(1:2) | 6.176 | 1.167 | 4.99 |
| IIP(1:3) | 6.176 | 1.547 | 4.61 |
| IIP(1:4) | 5.695 | 3.932 | 1.75 |
| IIP(1:5) | 5.695 | 4.393 | 1.29 |

The formation of the complex prior to the polymerization process is one of the key factors influencing adsorption performance. When the template ion–ligand complex is formed, specific recognition sites within the polymer are simultaneously established. This complex governs the spatial arrangement and orientation of the functional groups in the polymer matrix (Girija, 2022). The ratio of template ions to ligands determines the number of complexes formed. In the case of the Fe(III)–EDTA complex, each mole of EDTA forms a stable complex with one mole of the metal cation (Hafer et al., 2020). When Fe(III) ions fail to form complexes with EDTA, they are not incorporated into the polymer matrix, resulting in fewer specific binding sites. The unbound EDTA contributes to the formation of non-selective binding sites, resembling those present in the blank (non-imprinted) polymer (Laatikainen et al., 2015).

## Characterization using FTIR

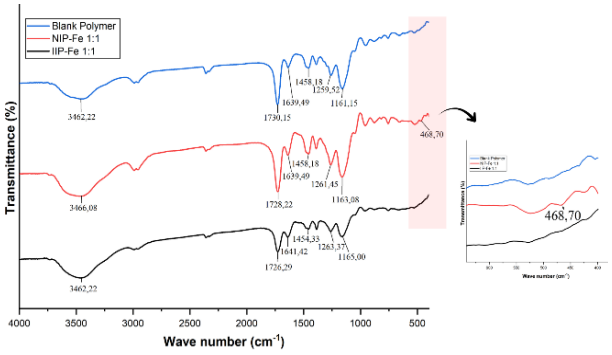


**Figure 1.** Spectrum FTIR blank polymer, NIP, and IIP

The FTIR spectra of the blank polymer, NIP, and IIP are illustrated in Fig. 1. Comparative analysis of these spectra revealed a notable distinction at the wavenumber of 486.70 $cm^{-1}$, which corresponds to the Fe–O bond observed in the NIP (Kiew et al., 2023). The absence of this characteristic peak in the IIP spectrum confirms the successful synthesis of the imprinted polymer. Furthermore, absorption bands appearing at 3462.22 and 3466.08 $cm^{-1}$ are associated with O–H stretching vibrations of carboxylic groups originating from EDTA and MAA, indicating the presence of hydroxyl functionalities in the polymer matrix. Additional bands detected at 1259.52, 1261.45, and 1263.37 $cm^{-1}$ were assigned to C–N stretching vibrations of EDTA. (Nandiyanto et al., 2023). Strong peaks at 1730.15, 1728.22, and 1726.29 $cm^{-1}$ were assigned to C=O stretching vibrations of ester groups from MAA and EGDMA, indicating the successful formation of ester linkages during the copolymerization process (Wirawan et al., 2019). The bands appearing at 1639.49 and 1641.42 $cm^{-1}$ correspond to the C=C stretching modes associated with the MAA and EGDMA monomer units (Bunina et al., 2017), while peaks at 1458.18 and 1454.33 $cm^{-1}$ represented additional C=C stretching vibrations from EGDMA, corresponding to the polymer backbone (Permatasari & Sianita, 2025). Peaks observed at 1161.15, 1163.08, and 1165.00 $cm^{-1}$ were attributed to C–O stretching vibrations from EGDMA, confirming the presence of ester structures in the polymer matrix (Bivián-Castro et al., 2023). Overall, these FTIR results confirm the successful synthesis of the Ion-Imprinted Polymer (IIP) incorporating MAA, EGDMA, BPO, and EDTA as active components.

## Characterization using SEM-EDX

The morphological characterization using SEM at a magnification of 20,000×, as shown in Figure 2, reveals distinct differences among the samples. The surface morphology of the blank polymer exhibits pores that are not clearly visible. The blank polymer was used as a reference and synthesized without the template ion; thus, it did not undergo the ion imprinting process that creates specific cavities for the target ion. The NIP displays a more irregular and slightly porous surface compared to the blank polymer. In contrast, the IIP shows a more porous surface with evident pore structures, indicating the presence of specific recognition cavities (imprinted cavities). The formation of these well-defined cavities arises from the removal of Fe(III) ions during the leaching stage. These cavities within the polymer matrix function as specific binding sites for Fe(III) ions.

EDX analysis confirmed that the blank polymer, NIP, and IIP all contained carbon and oxygen as the primary constituents of the polymer framework. However, iron was also detected in both the NIP and IIP samples. The IIP exhibited a lower iron content (0.36%) compared to the NIP (0.52%), which is attributed to the leaching process. The detection of these elements further verifies the successful synthesis of both NIP and IIP.

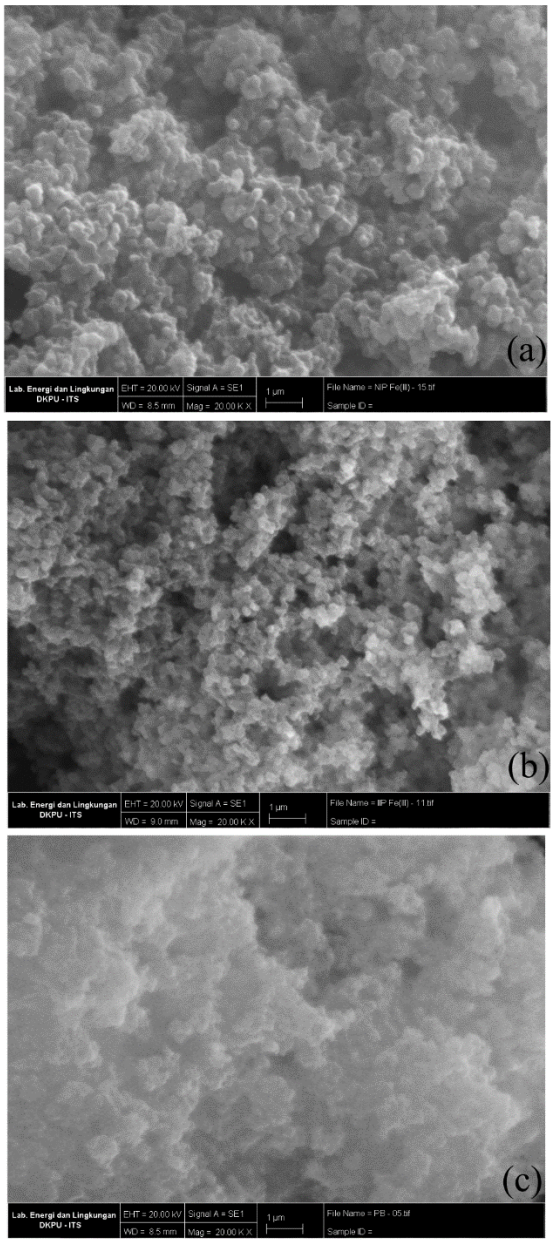


**Figure 2.** SEM of (a) NIP (b) IIP (c) blank polymer at 20.000x magnification.

## Fe(III)/Cr(III) Selectivity

Table 3 summarizes the distribution ratios (K) for IIP. In the selectivity test of the IIP, Cr(III) ions were chosen as competitor ions because Fe(III) and Cr(III) possess similarly small ionic radius, 0.66 Å and 0.62 Å, respectively. As shown in Table 3, the selectivity results for Fe(III)/Cr(III) indicate a distribution ratio (Kd) for the target ion significantly higher than that of the competing ion, with a selectivity coefficient (k) value of 132.776. This finding demonstrates that the IIP exhibits high selectivity toward the target ion.

**Table 3.** Selectivity of IIP

| Value | IIP(1:1) |
|---|---|
| Qe $_{Fe(III)}$ (mg/L) | 0.866 |
| Qe $_{Cr(III)}$ (mg/L) | 0.076 |
| Cf $_{Fe(III)}$ (mg/L) | 0.566 |
| Cf $_{Cr(III)}$ (mg/L) | 6.582 |
| $K_{Cr(III)}^{Fe(III)}$ | 132.776 |

## CONCLUSION

The findings of this study confirm the successful synthesis of the Fe-ion-imprinted polymer (IIP-Fe), highlighting the critical role of the EDTA ligand in determining the adsorption performance of the polymer toward Fe(III) ions. Among the various compositions investigated, the polymer prepared with a 1:1 ratio of template ion to ligand exhibited the maximum adsorption capacity of 5,189 mg/g. This enhanced performance can be ascribed to the optimal balance between template and ligand, as an excess of unbound EDTA tends to produce non-selective binding sites, thereby diminishing the selectivity of Fe(III) adsorption. FTIR spectral analysis confirmed the successful formation of the imprinted polymer through the presence of characteristic functional groups such as Fe–O. Furthermore, SEM-EDX characterization revealed clear morphological distinctions between the NIP and the IIP, with the latter displaying a higher density of pores and cavities formed by the removal of Fe(III) ions, thus validating the imprinting process within the polymer matrix.

## REFERENCES


Abbasi, S., Roushani, M., Khani, H., Sahraei, R., & Mansouri, G. (2014). Synthesis and Application of Ion-Imprinted Polymer Nanoparticles for the Determination of Nickel Ions. *Spectrochimica Acta - Part A: Molecular and Biomolecular Spectroscopy*, *140*, 534–543. https://doi.org/10.1016/j.saa.2014.11.107

Bivián-Castro, E. Y., Zepeda-Navarro, A., Guzmán-Mar, J. L., Flores-Alamo, M., & Mata-Ortega, B. (2023). Ion-Imprinted Polymer Structurally Preorganized Using a Phenanthroline-Divinylbenzoate Complex with the Cu(II) Ion as Template and Some Adsorption Results. *Polymers*, *15*(5), 1–15. https://doi.org/10.3390/polym15051186

Bunina, Z. Y., Bryleva, K., Yurchenko, O., & Belikov, K. (2017). Sorption Materials Based on Ethylene Glycol Dimethacrylate and Methacrylic Acid Copolymers for Rare Earth Elements Extraction from Aqueous Solutions. *Adsorption Science and Technology*, *35*(5–6), 545–559. https://doi.org/10.1177/0263617417701455

Cao, P., Pichon, V., Dreanno, C., Boukerma, K., & Delaunay, N. (2024). Use of the Dummy Approach for the Synthesis of Ion Imprinted Polymers with Ni(II) or Zn(II) as Template Ion for the Solid-Phase Extraction of Cu(II). *Journal of Separation Science*, *47*(6). https://doi.org/10.1002/jssc.202300891

Fei, Y., & Hu, Y. H. (2022). Design, Synthesis, and Performance of Adsorbents for Heavy Metal Removal from Wastewater: A Review. *Journal: Journal of Materials Chemistry A*, *10*(3), 1047–1085. https://doi.org/10.1039/D1TA06612A

Giove, A. (2024). *Preparation of Ion Imprinted Polymers for the Hydrometallurgical Separation of Co(II) and Ni(II) Ions : the Effect of Metal-Chelator Complexes on Selectivity* [Université de Toulon; Lappeenrannan-Lahden teknillinen yliopisto]. https://theses.hal.science/tel-04997704v1

Girija, P. (2022). General Characteristics and Applications of Ion Imprinted Polymers. *International Journal of Creative Research Thoughts (IJCRT)*, *10*(4), 2320–2882. www.ijcrt.org

Hafer, E., Holzgrabe, U., Kraus, K., Adams, K., Hook, J. M., & Diehl, B. (2020). Qualitative and Quantitative 1H NMR Spectroscopy for Determination of Divalent Metal Cation Concentration in Model Salt Solutions, Food Supplements, and Pharmaceutical Products by Using EDTA as Chelating Agent. *Magnetic Resonance in Chemistry*, *58*(7), 653–665. https://doi.org/10.1002/mrc.5009

Iacob, B.-C., Bodoki, A. E., Oprean, L., & Bodoki, E. (2018). Metal–Ligand Interactions in Molecular Imprinting. In *Ligand*. InTech. https://doi.org/10.5772/intechopen.73407

Ishak, N., Xin, T. C., Nasir, A. M., & Hoong, S. S. (2020). Optimization of Different Parameter in Synthesis Ion Imprinted Polymers via Precipitation Polymerization for Nitrate Adsorption. *IOP Conference Series: Materials Science and Engineering*, *864*(1). https://doi.org/10.1088/1757-899X/864/1/012184

Kiew, P. L., Ainaa, N., Shania, Lam, M. K., Tan, L. S., & Yeoh, W. M. (2023). Iron Oxide Nanoparticles Derived from Chlorella Vulgaris Extract: Characterization and Crystal Violet Photodegradation Studies. *Progress in Energy and Environment*, *24*(1), 1–10. https://doi.org/10.37934/progee.24.1.110

Kusumaningsih, D. I. P., Sudarni, D. H. A., & Wahyuningsih, S. (2022). Optimasi Pengaruh Waktu Kontak dan Dosis Adsorben Limbah Daun Kayu Putih (Melaleuca cajuputi) dengan Metode Isoterm Adsorpsi Langmuir. *Jurnal Teknik Kimia USU*, *11*(2), 72–79. https://talenta.usu.ac.id/jtk

Laatikainen, K., Udomsap, D., Siren, H., Brisset, H., Sainio, T., & Branger, C. (2015). Effect of Template Ion-Ligand Complex Stoichiometry on Selectivity of Ion-Imprinted Polymers. *Talanta*, *134*, 538–545. https://doi.org/10.1016/j.talanta.2014.11.050

Macena, M., Pereira, H., Cruz-Lopes, L., Grosche, L., & Esteves, B. (2025). Competitive Adsorption of Metal Ions by Lignocellulosic Materials: A Review of Applications, Mechanisms and Influencing Factors. In *Separations* (Vol. 12, Issue 3). Multidisciplinary Digital Publishing Institute (MDPI). https://doi.org/10.3390/separations12030070

Nandiyanto, A. B. D., Ragadhita, R., & Fiandini, M. (2023). Interpretation of Fourier Transform Infrared Spectra (FTIR): A Practical Approach in the Polymer/Plastic Thermal Decomposition. *Indonesian Journal of Science and Technology*, *8*(1), 113–126. https://doi.org/10.17509/ijost.v8i1.53297

Permatasari, Y., & Sianita, M. M. (2025). Optimization of pH Conditions for Lead Adsorption using Ion-Imprinted Polymer (IIP) with EDTA as Ligand. *IJCA (Indonesian Journal of Chemical Analysis)*, *8*(1), 31–39. https://doi.org/10.20885/ijca.vol8.iss1.art3

Pramastuti, F. R., Supriyantini, E., Pramesti, R., Sedjati, S., & Ridlo, A. (2024). Kitosan sebagai Bioadsorben Logam Besi (Fe) pada Jaringan Lunak Kerang Hijau (Perna viridis). *Buletin Oseanografi Marina*, *13*(1), 63–69. https://doi.org/10.14710/buloma.v13i1.41095

Rahman, I., Wahab, M. A., Akter, M., & Mahanta, T. R. (2024). Iron in Drinking Water and its Impact on Human Health –A Study in Selected Units of Jalalabad Cantonment. *Bangladesh Armed Forces Medical Journal*, *56*(2), 58–64. https://doi.org/10.3329/bafmj.v56i2.73013

Raji, Z., Karim, A., Karam, A., & Khalloufi, S. (2023). Adsorption of Heavy Metals: Mechanisms, Kinetics, and Applications of Various Adsorbents in Wastewater Remediation—A Review. *Waste*, *1*(3), 775–805. https://doi.org/10.3390/waste1030046

Salisna, Rasyid, N. Q., & Rianto, Muh. R. (2021). Kandungan Logam Besi pada Air Sumur Bor Di Muara Sungai Tallo Kota Makassar. *Jurnal Medika: Media Ilmiah Analis Kesehatan*, *6*(1), 6–9. https://doi.org/http://dx.doi.org/10.53861/jmed.v6i1.190

Wirawan, T., Supriyanto, G., & Soegianto, A. (2019). Preparation of a New Cd(II)-Imprinted Polymer and its Application to Preconcentration and Determination of Cd(ii) Ion from Aqueous Solution by SPE-FAAS. *Indonesian Journal of Chemistry*, *19*(1), 97–105. https://doi.org/10.22146/ijc.27703

Zhou, Z., Kong, D., Zhu, H., Wang, N., Wang, Z., Wang, Q., Liu, W., Li, Q., Zhang, W., & Ren, Z. (2017). Preparation and Adsorption Characteristics of an Ion-Imprinted Polymer for Fast Removal of Ni(II) Ions from Aqueous Solution. *Journal of Hazardous Materials*, *341*(2018), 355–364. https://doi.org/10.1016/j.jhazmat.2017.06.010